Substitutions of aspartic acid for glycine-220 and of arginine for glycine-664 in the triple helix of the proα1(I) chain of type I procollagen produce lethal osteogenesis imperfecta and disrupt the ability of collagen fibrils to incorporate crystalline hydroxyapatite

Ainsley A. CULBERT,* M. Philip LOWE,* Mary ATKINSON,† Peter H. BYERS,† Gillian A. WALLIS* and Karl E. KADLER*‡

*University of Manchester, School of Biological Sciences, Stopford 2.205, Oxford Road, Manchester M13 9PT, U.K., and †Departments of Pathology and Medicine, University of Washington, Seattle, WA 98195, U.S.A.

We identified two infants with lethal (type II) osteogenesis imperfecta (OI) who were heterozygous for mutations in the *COL1A1* gene that resulted in substitutions of aspartic acid for glycine at position 220 and arginine for glycine at position 664 in the product of one *COL1A1* allele in each individual. In normal age- and site-matched bone, ≈ 70% (by number) of the collagen fibrils were encrusted with plate-like crystallites of hydroxyapatite. In contrast, ≈ 5% (by number) of the collagen fibrils in the probands' bone contained crystallites. In contrast with normal bone, the *c*-axes of hydroxyapatite crystallites were sometimes poorly aligned with the long axis of fibrils obtained from OI bone. Chemical analysis showed that the OI samples contained normal amounts of calcium. The probands' bone samples contained type I collagen, overmodified type I collagen and elevated levels of type III and V collagens. On the basis of biochemical and morphological data, the fibrils in the OI samples were co-polymers of normal and mutant collagen. The results are consistent with a model of fibril mineralization in which the presence of abnormal type I collagen prevents normal collagen in the same fibril from incorporating hydroxyapatite crystallites.

INTRODUCTION

Osteogenesis imperfecta (OI), a heterogeneous group of dominantly inheritable disorders characterized by brittleness of bone, is caused by mutations in the *COL1A1* and *COL1A2* genes that encode the chains of type I collagen [1]. More than 100 mutations have been characterized in individuals with OI, including deletions, insertions, premature stop codons and single base substitutions [2], but how these mutations alter the structure of the collagen molecule and lead to bone fragility in OI remains poorly understood. The most common mutations are single base substitutions that change a codon for glycine to a codon for another amino acid in the triple-helical domain of the collagen molecule. The triple helix of type I collagen is comprised of three polypeptide chains, two α1(I) and one α2(I) chains, each constructed from a repeating Gly-Xaa-Yaa triplet, in which Xaa and Yaa can be any amino or imino acid (except tryptophan or cysteine). Glycine, with its small side chain, is essential at every third residue position for triple-helix formation.

Type I collagen is synthesized as a soluble precursor, procollagen, containing globular propeptides at the ends of each α chain. The procollagen is formed by trimerization of C-propeptides, and propagation of the triple helix occurs in a C-to-N-terminal direction (for a review see [2]). Cleavage of the propeptides by specific procollagen metalloproteinases generates the collagen that self-assembles into the fibrils that are the major source of mechanical strength of connective tissue and which form a template for matrix deposition. In bone, the fibrils are a template for mineralization in which crystallites of hydroxyapatite become incorporated into the fibril. The mechanical properties of bone, therefore, are dependent on an intimate association between the collagen fibrils and the crystallites of hydroxyapatite.

We have shown that two infants with lethal (type II) OI were heterozygous for mutations in the *COL1A1* gene that resulted in the substitution of aspartic acid for glycine-220 (^{G220D}) and arginine for glycine-664 (^{G664R}) in one or both of the proα1(I) chains of some type I procollagen molecules. The type I collagen was a mixture of normal and abnormal molecules and the abnormal molecules were post-translationally overmodified from the site of the substitution to the N-terminus of the triple helix. The abnormal collagen co-assembled with the normal collagen to form fibrils that were apparently as stable and as structurally intact as fibrils occurring in normal bone. However, in contrast with normal bone, in which about seven out of ten fibrils were encrusted in crystallites of hydroxyapatite, about nine out of ten fibrils in OI bone were completely free of crystallites of hydroxyapatite. Furthermore, the OI bone of a further individual with OI-II contained normal and overmodified type I collagen, elevated levels of type III and V collagens and mostly non-mineralized fibrils. The results add to a growing body of evidence that mutations in collagen genes that cause OI can result in collagen fibrils with impaired mineral-binding properties.

METHODS

Clinical histories

Proband 1 was the first pregnancy for a non-consanguineous couple. A tentative diagnosis of OI type 2 (OI-II) was made at approx. 18 weeks gestation on the basis of ultrasound studies. The parents elected to maintain the pregnancy, and a child with OI-II was delivered at 37 weeks gestation and died within 2 h of

Abbreviations used: OI (-II), osteogenesis imperfecta (type II); pN collagen, intermediate in the normal processing of type I procollagen to type I collagen containing the N-propeptides but not the C-propeptides; α chains, the chains of collagen; proα chains, the chains of procollagen; EM, transmission electron microscopy; ED, electron diffraction; DMEM, Dulbecco–Vogt Modified Eagle Medium; SSCP, single-strand-conformation polymorphism; RT-PCR, reverse transcription–PCR.

‡ To whom correspondence should be addressed.

birth. The radiographs are consistent with the diagnosis of OI-II. Dermal fibroblasts cultured from the affected infant synthesized normal and abnormal molecules, consistent with heterozygosity for a mutation in one type I collagen gene.

Proband 2 was the fourth pregnancy for a non-consanguineous couple. They had two living and well children; the third pregnancy resulted in a spontaneous miscarriage at 4 months gestation. Evaluation at 31 weeks gestation indicated the presence of short-limbed dwarfism. The infant was delivered at 38 weeks gestation and died in the immediate perinatal period. Radiographs and autopsy were consistent with lethal OI. Cultured fibroblasts from the foetus synthesized normal and abnormal type I collagen molecules, consistent with heterozygosity for a mutation in one of the type I collagen genes.

Proband 3 was the second pregnancy for a 25-year-old woman. Her first pregnancy had resulted in a term infant with O-II characterized by broad ribbon-like bone, multiple fractures of the limbs and ribs and an extremely soft calvarium. The infant died in the perinatal period. The second pregnancy, with a different partner, was identified to have short limbs, bowing and multiple fractures at 26 weeks gestation, and an elective termination was performed. Radiographic examination was consistent with the diagnosis of OI-II. Biochemical evaluation of fibroblasts cultured from the foetus indicated the presence of some normal molecules and some abnormal molecules, consistent with heterozygosity for a mutation in one of the type I collagen genes. The mutation has not yet been identified. Fibroblasts cultured from the mother synthesized only normal molecules. On the basis of biochemical and genetic evidence, the mother is apparently mosaic for the mutation identified in her children.

Sources of materials

Avian-myeloblastosis-virus reverse transcriptase, *Taq* DNA polymerase, nucleotides and restriction enzymes were from Boehringer; [^{14}C]formaldehyde was from New England Nuclear; [^{32}P]dCTP was from ICN–Flow; Sequenase PCR Product Sequencing Kit was from Amersham International; spectroscopically pure carbon (rods) and copper grids were from Agar Scientific (Stansted, Essex, U.K.); XAR-5 X-ray film from Kodak; water used in the preparation of samples for transmission electron microscopy (EM) and analyses of the proteins was from a commercial water-purification system that comprised tap water feeding into a Millipore RO6 Plus cartridge pack (Millipore) connected in-line to a Millipore Milli-Q Plus Ultra Pure water-purification system for final delivery.

Bone

Bone from femurs was collected at autopsy from three individuals with OI-II and frozen hydrated. Control bone was obtained from the rib and femur of two infants both of term gestation, delivered at 40 and 38 weeks respectively, whose cause of death was not a connective-tissue disorder. All bone samples were stored at −20 °C.

Extraction and radiolabelling of collagen from bone

Samples were thawed, cancellous bone and soft tissues removed, and pieces generated that were ≈ 8 mm^3. Between five and ten pieces of each sample were plunged into liquid nitrogen, powdered in a liquid-nitrogen-cooled bomb and resuspended in water. PMSF (1 mM), *N*-ethylmaleimide (10 mM) and *p*-aminobenzamidine (1 mM) were added. The suspension was dialysed for 20 h against 2 × 1 litre of 50 mM Tris/HCl buffer (pH 7.5 at 20 °C) containing 500 mM EDTA. The residue was free of mineral as shown by optical-microscopic examination of von Kossa-stained samples. Demineralized bone was either dialysed for 20 h against 2 × 1 litre of deionized water and freeze-dried or washed in deionized water and freeze-dried. Collagen was solubilized from the freeze-dried powder by pepsin (1 mg of pepsin/10 mg of demineralized bone) in 0.5 M acetic acid (pH 2). The sample was centrifuged, and the supernatant (which contained the pepsinized collagen) was neutralized with 1 M Tris/HCl buffer (pH 8 at 20 °C). Type I molecules were precipitated with 2.6 M NaCl, pH 7.4. Type V collagen was precipitated with 4.5 M NaCl, pH 7.4. Total collagens were precipitated with 4.5 M NaCl, pH 7.4. Collagens were radiolabelled by reductive methylation based on a method described previously [3]. In brief, samples were dialysed against 20 mM sodium cyanoborohydride in 0.15 M sodium tetraborate buffer, pH 8.0, and 50 μCi of [^{14}C]formaldehyde was added to the samples and incubated at room temperature overnight. To remove unincorporated formaldehyde, samples were dialysed against 0.1 M sodium phosphate buffer, pH 7.

SDS/PAGE

Proteins were analysed by discontinuous SDS/PAGE (5% separating gel and 3.5% stacking gel) and [^{14}C]formaldehyde-labelled collagens were detected by fluorography by exposing dried gels to pre-flashed Kodak XAR film at −70 °C [4]. Relative proportions of types I, III and V collagen in preparations were determined from densitometric scans (using a 2202 Ultroscan laser densitometer) of the α1(I), α1(III) and α1(V) chains of type I, III and V collagens respectively in fluorograms of gels run under delayed reduction [5]. Exposure times were adjusted to give intensities < 2 absorbance units to ensure a linear response of the photographic emulsion. Values were adjusted for the number of lysine residues in each chain and the number of α1 chains present in one molecule of each collagen type.

CNBr peptide mapping

CNBr treatment of ^{14}C-labelled proteins in gels and the separation of peptides in a second-dimension gel was performed as described in [6]. Peptides were revealed by fluorography as described above.

Preparation of bone for EM

Samples were pounded in a liquid-nitrogen-cooled bomb and the resultant powder was resuspended in 4 ml of ultra-pure water [R (resistance) = 18.2 M$\Omega \cdot$cm^{-1}]. Samples were homogenized, sonicated for 2 min (until a milky suspension was obtained) and centrifuged at 13000 g for 6 min. Pellets were resuspended in 100 μl of ultra-pure water and clarified by centrifugation at 13000 g for 5 s. The supernatant was drop-drained on to carbon-coated copper 600-mesh grids, washed twice with distilled water and air-dried. Grids were examined by EM using a JEOL 1200 EX instrument at an accelerating voltage of 100 kV. Images were recorded between × 5000 and × 30000 magnification using 5 cm × 9 cm AGFA EM film.

Electron-diffraction (ED) patterns from mineralized fibrils

The electron microscope was electron-optically aligned before operation in the diffraction mode [7]. The axis of the electron beam was aligned with the mechanical and optical axes of the EM column to maximize even illumination of the sample and to minimize distortion in the final image. A small-area selective aperture (diameter 20 μm) was used to exclude objects on the grid that could contribute to the diffraction pattern. The aperture

was inserted in the back focal plane of the objective lens. Only the portion of the specimen lying within this selected area contributed to the diffraction pattern. Evaporated aluminium was used to calibrate the diffraction patterns. EM images were recorded of the selected area of the mineralized fibrils from which the diffraction patterns were obtained. Image rotation (which occurs on switching the JEOL instrument between transmission and diffraction modes) was corrected using a molybdenum oxide test grid.

Analysis of the chemical composition of bone

Powdered cortical bone was freeze-dried and analysed for C, H, N, O and Ca content by the Microanalytical Laboratory in the Department of Chemistry of the University of Manchester.

RESULTS

Collagen composition of normal and OI bone

SDS/PAGE and fluorography of pepsin-treated and ^{14}C-labelled bone proteins showed that normal bone contained predominantly α1(I) and α2(I) chains of type I collagen, with minor contributions from α1(III) chains of type III collagen and α1(V) and α2(V) chains from type V collagen (see Figure 1 and Table 1).

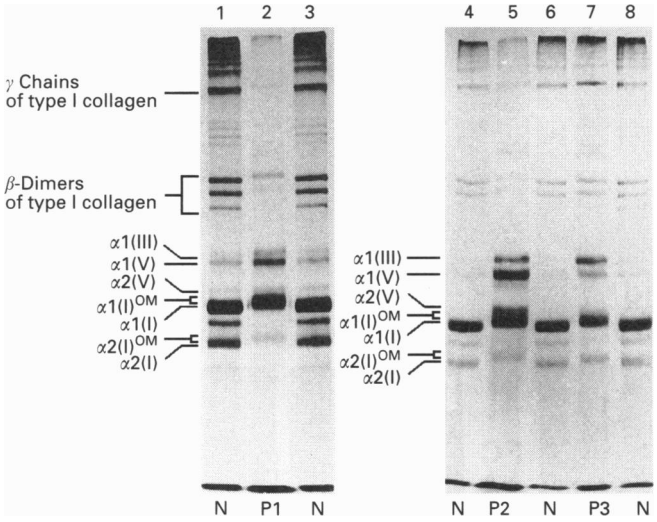

Figure 1 SDS/PAGE of collagen chains in normal and OI bone

^{14}C-labelled samples were examined by SDS/PAGE on a 5% gel and fluorography under delayed reduction. Lanes 1, 3, 4, 6 and 8, normal; lane 2, proband 1; lane 5, proband 2; lane 7, proband 3. The direction of migration is from top to bottom. N denotes normal samples, P1 denotes proband 1, P2 denotes proband 2, and P3 denotes proband 3. ^{OM} means overmodified chain.

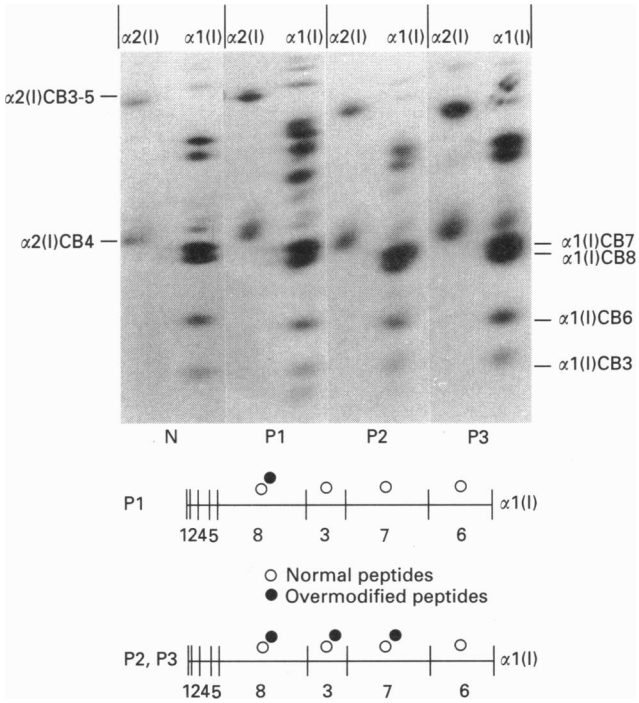

Figure 2 Analysis of CNBr peptides of type I collagen extracted from normal and OI bone

^{14}C-labelled α-chains were separated by SDS/PAGE in a 5% gel, cleaved in the gel slices with CNBr, and the peptides separated by SDS/PAGE in a 12.5% gel and examined by fluorography. N denotes normal samples, P1 denotes proband 1, P2 denotes proband 2 and P3 denotes proband 3. Overmodified α1(I) and α2(I) chains from probands 1, 2 and 3 yielded peptides that migrated more slowly than peptides derived from the normally migrating α1(I) and α2(I) chains. The CNBr peptides from the type I collagen extracted from normal bone migrated as single discrete spots.

SDS/polyacrylamide gels of bone from all three OI samples contained slowly migrating chains of type I collagen, and elevated levels of type III and V collagens with respect to the normal control bone examined (Table 1).

Analysis of CNBr peptides of normal and OI collagens from bone

To map the site of the mutation to a region of the collagen molecule and to illustrate the presence of overmodified collagen, samples of ^{14}C-labelled type I collagen from normal and OI bone (precipitated by 2.6 M NaCl, pH 7.4) were separated by SDS/PAGE and treated with CNBr in gels *in situ*. The resultant peptides were separated by two-dimensional SDS/PAGE and

Table 1 Percentage content of types I, III and V collagen in normal and OI bone samples

Values were obtained from densitometric scans of SDS/polyacrylamide gels by measurement of the relative intensities of the α1(I), α1(III) and α1(V) chains, after adjustment for lysine content and the homotrimeric composition of type III collagen.

Sample	Age of sample (weeks)	Type I collagen	Type III collagen	Type V collagen
Normal	Term (38)	97	< 1	2–3
Proband 1^{G220D}	Term (37)	81	5	14
proband 2^{G664R}	Term (38)	43	14	43
Proband 3	26–27	77	16	8

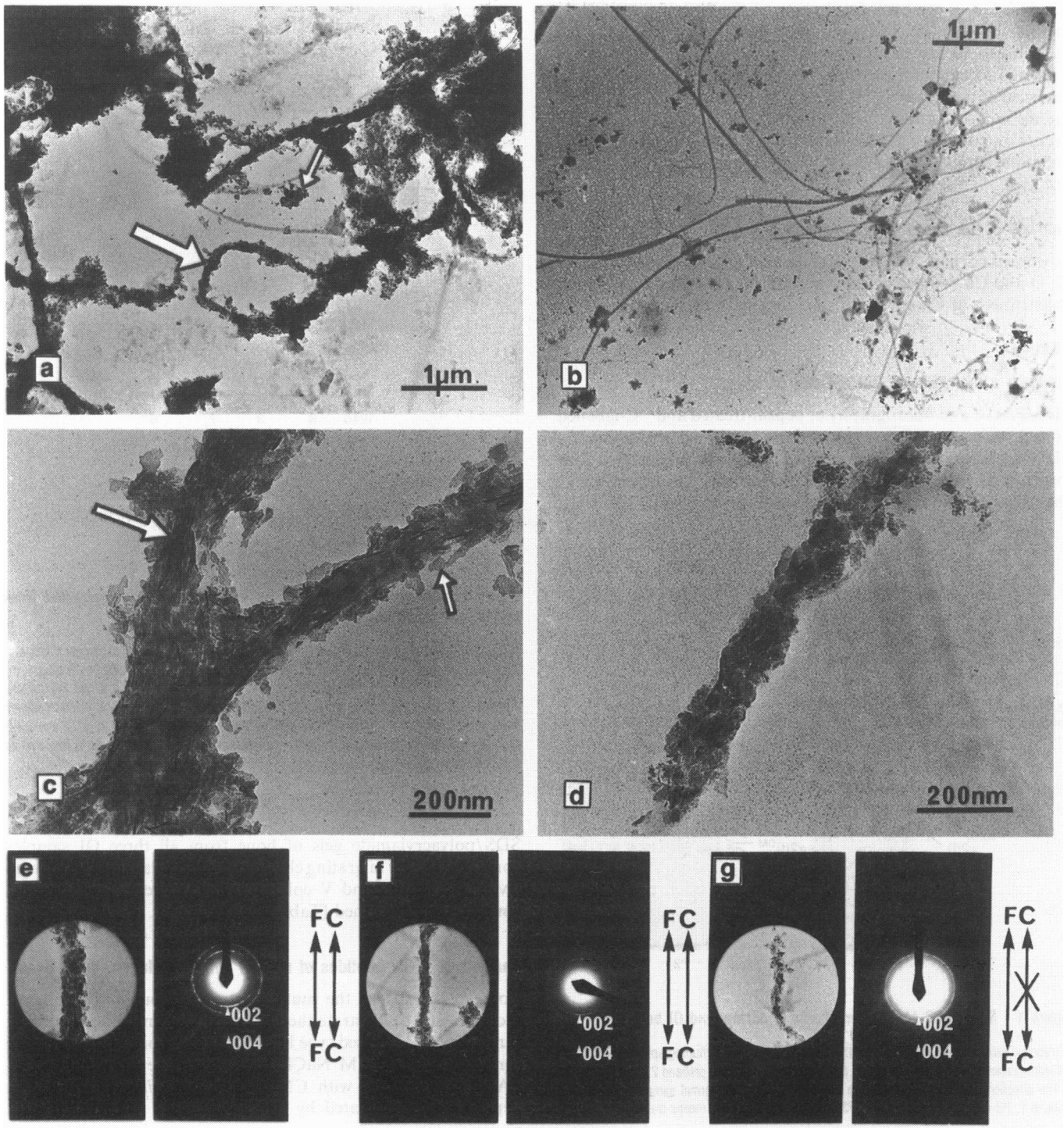

Figure 3 Analysis of normal and OI bone by EM and ED

Panels a–d, EM of normal and OI bone. Panels e–g, ED of mineralized fibril fragments obtained from normal and OI bone. Panel a, low-magnification image of fibril fragments from normal bone. The usual cross-striated pattern of the fibril is obscured by heavy deposits of hydroxyapatite crystallites. The large arrow indicates a mineralized fibril fragment. The small arrow shows free crystallites not associated with fibrils. Panel b, OI bone from proband 1. The fibrils are non-mineralized and exhibit the usual cross-striations of collagen fibrils. Free crystallites occur in the background not associated with fibrils. Panel c, high-magnification micrograph of a fragment from normal bone. The large arrow indicates crystallites in edge-on orientation. The small arrow indicates crystallites in face-on orientation. Panel d, high-magnification micrograph of fragments from OI bone showing a mineralized fibril. Panels e, f and g, left-hand panels indicate the selected area of the fibril fragments from which the diffraction patterns were taken. Right-hand panels illustrate the resulting diffraction patterns in which the 002 and 004 reflections are indicated. F denotes the long axis of the fibril and C denotes the *c*-axis of the unit cell of the hydroxyapatite crystals. Panel e, diffraction pattern obtained from a normal fibril fragment. The *c*-axes of the hydroxyapatite crystals are on average parallel with the long axis of the collagen fibril. Panels f and g, diffraction patterns obtained from fibril fragments from OI bone. The reflections were less intense than those seen from normal fibrils. The diffraction pattern in panel f indicates that the *c*-axes of the hydroxyapatite crystals are near-parallel with the long axis of the collagen fibril. The pattern in panel g indicates that the *c*-axes of the hydroxyapatite crystals are not well aligned with the long axis of the collagen fibril.

detected by fluorography. Chains in normal and OI samples gave rise to spots that were identified as α1(I) CB3, CB6, CB7 and CB8 and α2(I) CB4 and CB3-5. In proband 1 the α1(I) CB8 and α2(I) CB4 migrated as smears, indicating the presence of normal peptides and post-translationally overmodified peptides, and that the mutation resided in the either the α1(I) or α2(I) genes corresponding to the CB8 region of the molecule (residues 123–401). In probands 2 and 3, the CB3, CB7 and CB8 peptides migrated as smears indicative of the presence of normal and mutated type I collagen and a mutation in either the α1(I) or α2(I) genes corresponding to the CB7 region of the molecule (Figure 2).

Table 2 Chemical composition of normal and OI bone

Sample	Age of sample (weeks)	Composition (% of dry mass)			
		Ca	C	H	N
Normal	Term (38)	23.6	17.1	3.2	4.5
Proband 1^{G220D}	Term (37)	21.2	16.7	2.3	5.1
Proband 2^{G664R}	Term (38)	22.3	17.3	3.7	4.2
Proband 3	26–27	15.8	19.5	3.6	5.3

Localization and identification of the mutation

Probands 1 and 2 were selected for mutational analysis because dermal fibroblasts were available and grew well in culture.

Mutations in the collagen I genes of the probands were detected using standard techniques of reverse transcription–PCR (RT-PCR), single-strand-conformation polymorphism (SSCP) and DNA sequencing (results not shown). Proband 1 was heterozygous for a G-to-A transition in one of the *COL1A1* alleles that changed a codon for glycine-220 to a codon for aspartic acid. Proband 2 was heterozygous for a G-to-C transition in one of the *COL1A1* alleles that changed a codon for glycine-664 to a codon for arginine. The mutation in proband 1 disrupted a restriction-endonuclease-*Ban*I site in the DNA and the mutation in proband 2 disrupted a site for cleavage by *Eco*RII. Thus we were able to confirm the mutations by restriction analysis (results not shown).

EM of fibril fragments

Two grids for each of the OI probands and normal bone samples were examined. Each grid contained at least 500 fibril fragments. At low magnification of normal bone unstained for EM, a typical field contained fragments of collagen fibrils that were encrusted with crystallites of hydroxyapatite and plate-like crystals that were not associated with collagen fibrils (Figure 3, panel a). Non-mineralized fibrils (i.e. fibrils that did not contain crystallites over extended regions) accounted for ≈ 30% of the fibril fragments. In contrast, in bone from proband 1, most of the fibril fragments were free of crystallites and exhibited the usual cross-striation of collagen fibrils (Figure 3, panel b). At higher magnification (≈ 25000×) fibrils from normal bone contained crystallites that could be seen clearly in both 'edge on' and 'face on' orientations (see Figure 3, panel c). Crystallites in edge-on orientation were densely electron-opaque and appeared needle-shaped. Crystallites in face-on orientation were approximately rectangular with rough borders. A rare mineralized fibril from proband 1 was morphologically similar to those in normal bone, although the orientation of crystallites in OI fibrils was difficult to visualize (Figure 3, panel d).

ED from mineralized fibrils

Figure 3, panel e, shows a typical ED pattern obtained from 80 fibril fragments derived from normal bone. A distinctive feature of all the patterns was the occurrence of two discontinuous rings (or arcs). Measurement of the radius of the arcs was used to determine the lattice spacings. Comparison against evaporated aluminium as a reference standard and subsequent cross-reference against the entries in the chemical handbook of the American Society of Testing Materials showed that the arcs arose from the accumulative effect of multiple and near-aligned 002 and 004 reflections of the *c*-axis of the hydroxyapatite unit cell. A line drawn through the points of maximum intensity of these arcs was parallel with the long axis of the fibril.

ED patterns were obtained from 25 mineralized fibrils from OI bone. Fibrils from each of the OI probands were examined separately, the vast majority of which were from probands 1 and 2. Of the diffraction patterns, 20 exhibited reflections that originated from the 002 and 004 lattice planes. These data showed that the *c*-axes of the crystallites were parallel ± ≈ 30° to the long axis of the collagen fibril. Most of these patterns exhibited weaker reflections than those seen from normal crystallites (Figure 3, panel f). In other patterns from probands 1 and 2, the *c*-axis of the crystallites did not closely align with the long axis of the fibril (see Figure 3, panel g). It was noteworthy that fibrils giving rise to low-intensity diffraction patterns and patterns in which the crystal and fibril axes did not align were not observed from normal bone.

Analysis of the chemical composition of bone

The chemical composition of bone from proband 1 and 2 was indistinguishable from that of normal age-matched control bone (see Table 2). Bone from proband 3 had lower levels of Ca and elevated levels of C when compared with probands 1 and 2.

DISCUSSION

The picture that is emerging from studies of OI is that the manner in which mutations produce the lethal phenotype is complex. There are several interacting themes. Mutations can have a deleterious effect on transport through the cell of molecules that incorporate abnormal chains. This effect appears greatest for those mutations in the C-terminal half of the molecule and may be both mutation- and position-specific. Once secreted, many abnormal molecules are delayed in processing at their N-terminal ends by procollagen N-proteinase [8], indicating that these molecules probably have an abnormal structure. Because the ultimate effect of the mutation is in the extracellular matrix, especially in bone, understanding how the abnormal molecules perturb the formation of this complex matrix has become important. It is clear from our studies and those of others, that several factors contribute to abnormal bone formation in individuals with mutations in type I collagen genes. One explanation for the lethality of some glycine substitutions is that the presence of bulky charged side groups at a site normally occupied by a proton introduces into the triple helix a hydrated loop that may interfere with the folding of the triple helix and, thereby, its thermal and proteolytic stability. The molecules that contain the abnormal chains may be delayed in transit through the cell, while post-translational modification is increased and, ultimately, the efficiency with which those molecules are deposited outside the cell is less than that for the normal molecules. Once molecules containing the abnormal chains are in the matrix, however, a

proportion of the abnormal molecules participate in collagen fibril formation with normal collagen molecules. It is striking that, although fibrils appear to be formed in a relatively normal fashion, mineralization of the fibrils is markedly defective, with virtually no crystallites apparent on the vast majority of fibrils isolated from the abnormal bone. Chemical analysis showed that the content of Ca, C, H and N in the bone of probands $1^{(G220D)}$ and $2^{(G664R)}$ was indistinguishable from that in normal age-matched controls. Other studies have also noted that the amount of inorganic material in bone did not vary significantly between OI patients and control bone [9,10]. Our results suggested that the absence of mineralized fibrils was not simply a result of decreased Ca levels. Rather, the results suggest that the presence of mutated collagen molecules within the fibrils inhibits mineralization. Supposedly, non-mineralized fibrils cannot provide any of the usual properties of bone necessary to resist deformation produced by muscular tone and other forces.

The manner in which abnormal collagen interferes with mineralization is not yet clear, and many factors may play a role. In addition to normal and abnormal type I collagen, the collagen fibrils in bone from all three probands contained elevated levels of type III and V collagen. In proband 2, type V collagen accounted for 43% of the collagen in the matrix. The accumulation of the collagen types III and V in bone from infants with OI type II has been noted previously [11,12]; subsequent *in vivo* and *in vitro* studies showed that both types of collagen can assemble with type I collagen into fibrils [13–18]. These data, in sum, suggest that collagens type III and V may assemble with type I collagen in the abnormal bone and may contribute to defects in mineralization.

Although there is no direct evidence for the co-assembly of normal and abnormal type I collagen in OI fibrils, two lines of evidence support this possibility. First, non-mineralized fibrils accounted for 95% of the fibrils present in the OI samples. If normal and abnormal collagen molecules had occurred in separate fibrils, then many more mineralized fibrils might have been expected to occur, consonant with the proportion of normal type I collagen molecules in the fibril as a whole. Moreover, abnormal and normal molecules occurring at different sites along the same fibril might have been expected to produce fibrils that were partially mineralized. Secondly, CNBr fragmentation and SDS/PAGE analysis of preparations of OI fibrils from three affected individuals contained overmodified and normal type I collagen.

The presence of non-mineralized fibrils in bone from individuals with OI has been noted by Traub and co-workers [19] and by Cohen-Solal et al. [20] recently. Traub and co-workers observed regions of loose non-mineralized fibrils in bone from individuals with OI; other regions of the bone appeared over-mineralized where crystallites were deposited on to fibril surfaces or in separate clusters. Cohen-Solal et al. [20], in their study of an infant with lethal OI, observed that the mineralizing front of bone contained few fibrils and that those fibrils were not associated with mineral. These small numbers of studies of fibril morphology and mineralization begin to suggest that fibril mineralization may be the common theme by which to understand the pathophysiology of OI. The irregular arrangement of crystallites in some fibrils suggests that decreased mineralization may reflect an abnormal fibril template. Studies with procollagen N-proteinase suggest that substitutions for glycine within the triple helix may introduce loops [21], phase shifts and changes in the pitch of the triple helix of the procollagen molecule, and, in some molecules containing substitutions of cysteine for glycine, kinks [8]. All of these disruptions could affect the lateral association of molecules into fibrils. Secondly, the mutations which result in abnormal helix structure also result in post-translational overmodification of chains N-terminal to the site of the mutation. In those molecules, highly hydrated side chains of O-linked glycosides might further interfere with the packing and, themselves, may disrupt the organization of mineral crystallites. Finally, the presence of increased amounts of type III and type V collagen in fibrils may provide additional constraints on orderly mineralization. Thus it appears that even the presence of a relatively small number of abnormal molecules [22] may have the capacity to disable almost completely the intricate system of bone formation.

Received 30 January 1995/13 May 1995; accepted 22 June 1995

This work was supported by grants from Action Research (S/P/2355), the Wellcome Trust (19512) and the National Institutes of Health (AR21557, AR41223). K.E.K. is a recipient of a Senior Research Fellowship award in Basic Biomedical Science from the Wellcome Trust.

REFERENCES

1 Chessler, S. D., Wallis, G. A. and Byers, P. H. (1993) J. Biol. Chem. **268**, 18218–18225
2 Kadler, K. E. (1994) Protein Profile **1**, 519–638
3 Dottavio-Martin, D. and Ravel, J. M. (1989) Anal. Biochem. **87**, 562–565
4 Kadler, K. E., Hojima, Y. and Prockop, D. J. (1987) J. Biol. Chem. **262**, 15696–15701
5 Sykes, B, Puddle, B., Francis, M. and Smith, R. (1976) Biochem. Biophys. Res. Commun. **72**, 1472–1480
6 Bonadio, J., Holbrook, K. A., Gelinas, R. E., Jacob, J. and Byers, P. H. (1985) J. Biol. Chem. **260**, 1734–1742
7 Weakley, B. S. (1981) Biological Transmission Electron Microscopy, pp. 195–211, Churchill–Livingstone, Edinburgh
8 Lightfoot, S. J., Holmes, D. F., Brass, A., Grant, M. E., Byers, P. H. and Kadler, K. E. (1992) J. Biol. Chem. **267**, 25521–25528
9 Sokolov, B. P., Sher, B. M.., Hausmann, J., Marik, I., Deyl, Z. and Kalinin, V. N. (1992) Biochim. Biophys. Acta **1138**, 93–96
10 Brenner, R. E., Vetter, U., Nerlich, A., Worsdorfer, O. and Teller, W. M. (1989) Eur. J. Clin. Invest. **19**, 159–166
11 Bateman, J. F., Chan, D., Mascara, T., Rogers, J. G. and Cole, W. G. (1986) Biochem. J. **240**, 699–708
12 Pope, F. M., Nicholls, A. C., Eggleton, C., Narcissi, P., Hey, E. N. and Parkin, J. M. (1980) J. Clin. Pathol. **33**, 534–538
13 Becker, J., Schuppan, D., Rabanus, J. P., Rauch, R., Niechoy, U. and Gelderblom, H. R. (1991) J. Histochem. Cytochem. **39**, 103–110
14 Fleischmajer, R., Perlish, J. S., Burgeson, R. E., Shaikh Bahai, F. and Timpl, R. (1990) Ann. N. Y. Acad. Sci. **580**, 161–175
15 Fleischmajer, R., Perlish, J. S., Timpl, R. and Olsen, B. R. (1988) J. Histochem. Cytochem. **36**, 1425–1432
16 Romanic, A. M., Adachi, E., Kadler, K. E., Hojima, Y. and Prockop, D. J. (1991) J. Biol. Chem. **266**, 12703–12709
17 Adachi, E. and Hayashi, T. (1986) Connect. Tissue Res. **14**, 257–266
18 Birk, D. E., Fitch, J. M., Babiarz, J. P., Doane, K. J. and Linsenmajer, T. F. (1990) J. Cell Sci. **95**, 649–657
19 Traub, W., Arad T., Vetter, U. and Weiner, S. (1994) Matrix Biol. **14**, 337–345
20 Cohen-Solal, L., Zylberberg, L., Sangalli, A., Lira, M. G. and Mottes, M. (1994) J. Biol. Chem. **269**, 14751–14758
21 Bella, J., Eaton, M., Brodsky, B. and Berman, H. M. (1994) Science **266**, 75–81
22 Stacey, A., Bateman, J., Choi, T., Mascara, T., Cole, W. and Jaenisch, R. (1988) Nature (London) **332**, 131–136